

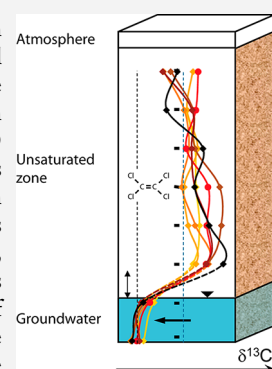
Can Soil Gas VOCs be Related to Groundwater Plumes Based on Their Isotope Signature?

S. Jeannotat and D. Hunkeler*

Centre for Hydrogeology & Geothermics (CHYN), University of Neuchatel, Rue Emile Argand 11, CH-2000 Neuchatel, Switzerland

Supporting Information

ABSTRACT: The isotope evolution of tetrachloroethene (PCE) during its transport from groundwater toward the soil surface was investigated using laboratory studies and numerical modeling. During air–water partitioning, carbon and chlorine isotope ratios evolved in opposite directions, with a normal isotope effect for chlorine ($\epsilon = -0.20\text{‰}$) and an inverse effect for carbon ($\epsilon = +0.46\text{‰}$). During the migration of PCE from groundwater to the unsaturated zone in a 2D laboratory system, small shifts of carbon and chlorine isotope ratios ($+0.8\text{‰}$) were observed across the capillary fringe. Numerical modeling showed that these shifts are due to isotope fractionation associated with air–water partitioning and gas-phase diffusion. Carbon and chlorine isotope profiles were constant throughout the unsaturated zone once a steady state was reached. However, depending on the thickness of the unsaturated zone and its lithology, depletion in heavy isotopes may occur with distance during the transient migration of contaminants. Additionally, variations of up to $+1.5\text{‰}$ were observed in the unsaturated zone for chlorine isotopes during water table fluctuations. However, at steady state, it is possible to link a groundwater plume to gas-phase contamination and/or to differentiate sources of contamination based on isotope ratios.



INTRODUCTION

Chlorinated compounds found in the environment are often released at or near the land surface as a dense nonaqueous-phase liquid (DNAPL). DNAPLs can then migrate vertically (depending on gravity and capillary forces) through the unsaturated zone to reach underlying aquifers.¹ After penetrating the aquifer they tend to form pools over low permeability geological layers and, as their solubility in water is generally low, create long-term groundwater contamination.² Chlorinated ethenes can volatilize from groundwater and then migrate by diffusion, which is the most significant transport process in the gas phase,^{3,4} through the unsaturated zone to the soil surface. Moreover, a certain amount of NAPLs can be retained in the unsaturated zone during the migration of NAPLs through the soil (2–20% of the available pore space⁵), and create a persistent source of contamination. Due to their high vapor pressure, chlorinated compounds vaporize, creating a vapor-phase contaminant plume.^{3,6–9} Chlorinated ethenes are transported away from the NAPL source by gaseous diffusion and may induce groundwater contamination even if the NAPL has not reached the water table.¹⁰ Mass transport between unsaturated and saturated zones and inside the unsaturated zone thus plays an important role in controlling the fate of these contaminants.¹¹

Stable isotope analysis is increasingly used to investigate the behavior of organic or inorganic contaminants in the subsurface. Compound-specific isotope analysis (CSIA) has proven to be an effective tool to distinguish between different contaminant sources and to relate contaminant plumes to their source.^{12–15} CSIA was also used to demonstrate and quantify in situ biodegradation of petroleum hydrocarbons and chlorinated

solvents in groundwater.^{16–19} There is also an increasing interest to apply CSIA in unsaturated zone studies to relate vapor-phase contamination in the unsaturated zone to NAPL sources or groundwater plumes and to demonstrate reactive processes. However, previous laboratory studies have suggested that, in the unsaturated zone, isotope ratios may also be influenced by transport and partitioning processes. Isotope fractionation was observed for diffusion of VOCs across a porous media, vaporization from a NAPL phase, and air–water partitioning.^{20–24} The studies of Bouchard et al.²² and Jeannotat and Hunkeler²⁴ have highlighted a depletion of heavy isotopes with distance from a source of hydrocarbons and trichloroethylene (TCE), respectively, during the initial expansion of a vapor plume that vanishes at steady state. Moreover, in the case of TCE, diffusion-controlled vaporization induces an enrichment of the heavy chlorine isotopes but a constant carbon isotopic ratio at the source of contamination, while in the case of hydrocarbons the carbon becomes enriched in the heavy isotopes. Kuder et al.²³ investigated the combined effect of air–water partitioning and vapor diffusion on carbon and hydrogen isotope ratios of MTBE during diffusive volatilization and air sparging of dissolved compounds using sand-filled columns. For carbon, no isotope fractionation was observed for air sparging while an isotope enrichment factor of -1.0‰ was reported for diffusive volatilization. For hydrogen, enrichment factors of -5 to -12‰ were observed for diffusive

volatilization and air-sparging from aqueous solutions, respectively. A previous field and numerical study for a site where NAPL was present in a thick unsaturated zone suggested that constant isotope ratios from groundwater to the soil surface are only expected once a steady state is reached.²⁵ However, potential variations of isotope ratio during the transfer of contaminants from a groundwater contaminant plume across the capillary fringe to the unsaturated zone have not yet been studied experimentally. Hence it remains open if CSIA is suitable to relate contaminants present in the unsaturated zone to those in underlying groundwater plumes. Significant effects might especially occur for chlorine isotopes in chlorinated solvents due to the mass difference of two between isotopes (35 vs 37) and due to the smaller isotope variations of source material compared to carbon.

The main aim of this study is to investigate isotope fractionation during the migration of volatile organic compounds (VOCs) from groundwater across the capillary fringe and through the unsaturated zone toward the atmosphere using laboratory studies and numerical modeling. Tetrachloroethene (PCE) was used as a model compound. Carbon and chlorine isotopes were investigated together as in practical applications of a multi isotope approach is more promising to relate isotope variations to different sources and processes. Isotope fractionation during air–water partitioning was first evaluated in isolation using a multistep equilibration approach that excluded a contribution of diffusion to isotope fractionation. The effect of the transport of PCE from groundwater across the capillary fringe and through the unsaturated zone on the isotope ratios was then evaluated. For these studies, a 2D laboratory system with horizontal water flow in the bottom part rather than a classical column was used as the transfer of compounds across the capillary fringe depends on the groundwater flow rate. In a first experiment, steady-state flow conditions were established and the transient migration of PCE was investigated. In the second experiment, groundwater flow was also transient. As the PCE is stable under the oxic conditions typically encountered in sandy unsaturated zones,²⁶ it was possible to evaluate the effect of transport and partitioning processes in isolation, without any degradation. To generalize the results of the laboratory experiments and to study various scenarios, numerical modeling was also carried out. The numerical modeling makes it possible to gain additional insight into the physical processes influencing isotope fractionation. Based on the experimental and numerical study, it was finally possible to draw conclusions about the use of CSIA to fingerprint VOCs contamination under variably saturated conditions.

■ MATERIALS AND METHODS

Air–Water Partitioning. As a basis for the interpretation of the 2D laboratory experiment, it needs to be known how air–water partitioning influences isotope fractionation in isolation. The effect of air–water partitioning was investigated using a similar approach as the one previously developed by Jeannotat and Hunkeler.²⁴ The air–water partitioning experiments were carried out with a 50 mL gastight syringe partially filled with 30 mL of an aqueous solution of PCE at 5 mg/L with 20 mL of gas phase remaining. After an equilibration time of 20 min on a rotary shaker at 200 rpm in a horizontal position the gas phase was pushed out of the syringe and replaced by clean air. Experiments with an increasing number of equilibration steps ($n = 1–7$) were carried out and 20 mL of

the water was sampled after the last step of each experiment. The whole experimental procedure was repeated twice. As a previous study²⁴ has shown that isotope fractionation in such a multistep equilibration process follows in good approximation a Rayleigh distillation trend, the results of the experiments were plotted and evaluated using the following equations:

$$\ln[(\delta)/(\delta_i)] = (\alpha - 1)\ln f \quad (1)$$

$$\varepsilon = (\alpha - 1) \quad (2)$$

where δ is the isotopic composition of PCE for a particular value of f , δ_i is the initial isotopic composition of PCE, f is the fraction of liquid PCE remaining, α is the isotope fractionation factor, and ε is the isotope enrichment factor. The uncertainty associated with the isotope enrichment factor is characterized by the standard deviation of the slope of the linear regression.

Transport of PCE through the Capillary Fringe and the Unsaturated Zone.

The transfer of PCE from groundwater across the capillary fringe and the unsaturated zone was investigated in a 2D laboratory system at 25 °C. 2D laboratory systems have previously been used, e.g., to investigate oxygen transfer across the capillary fringe.²⁷ This 2D system was 0.07 m wide, 0.3 m long, and 0.8 m high, and was built mainly in stainless steel with a glass panel on one side to allow observation of variations of the water table. Sampling ports were installed in the center of the system at various heights along the model. Quartz sand (grain size of 0.7–1.2 mm) was packed inside the system. A gear pump was used to establish a pulse-free, horizontal water flow in the bottom of the model system. The experimental setup is illustrated in Figure S1 of the Supporting Information (SI). At the beginning of the experiment, the 2D system was completely filled with water from the bottom with the gear pump. Based on the volume of water added (6.2 L) and the total volume of the system (15.1 L), the porosity is estimated to be 0.41. Water was then removed from the system (5.1 L), and the setup was filled and emptied again in order to establish a typical drainage water saturation profile with a capillary fringe of 3–5 cm height based on visual observations.

Two different experiments were carried out. The first experiment was carried out under steady-state flow conditions with a constant water table set to 0.12 m using a constant-head reservoir at the outlet of the system (SI Figure S1) and a stable capillary fringe as indicated by visual observations. The horizontal water flow velocity of approximately 25 cm/day (1.05 mL/min) was maintained for two weeks in order to create stable hydraulic conditions. An oxic aqueous solution with PCE at saturation (210 ± 16 mg/L at 25 °C) prepared in a 5 L glass bottle was then circulated continuously through the 2D system in a closed loop with the outlet of the 2D system connected to the glass bottle. The glass bottle contained excess PCE NAPL and was stirred with a magnetic stirrer to ensure a constant PCE concentration. The upper part of the 2D system with a 5 cm thick headspace was tightly closed and flushed with clean humidified synthetic air at 15 mL/min to remove the gaseous PCE from the system and to maintain the humidity profile. As the resistance for gas flow in the headspace is very small, pressure gradients across the headspace were very small and hence no significant gas flow was induced in the porous media. The good agreement between measured and modeled concentrations confirms that this assumption is reasonable. Gas samples of 2 mL volume for concentration and isotope ratios analyses were taken with a gastight syringe at different heights

(0, 10, 20, 30, 40, 50, and 60 cm) in the center of the system after 1, 1.5, 2, 3, 4, 10, and 20 days. Steady-state flow conditions were maintained for 20 days at the end of the first experiment and before the beginning of the second study. The second study investigated the concentration and isotope evolution during water level fluctuations. Two gear pumps were used to increase or decrease the water table in the system; one at the inlet of the 2D system and one in the outlet. The outflow was set to the same flow rate as for the first experiment. To raise the water level the inflow rate was increased, and to drop the water level the inflow was reduced. The water table was first raised during 1.5 day from 0.12 to 0.25 m and stabilized for 3 days. The water level was then lowered back to 0.12 m in a period of 1.5 day and stabilized for 3 more days before a final increase of water table from 0.12 to 0.25 m. Under oxic condition in clean quartz sand, no biodegradation of PCE is expected to occur as confirmed by the absence of degradation products such as trichloroethene or dichloroethene.

Sample Storage and Analysis. Gaseous samples were dissolved into water as described in Jeannotat and Hunkeler.²⁴ Aqueous samples were found to be more stable for storage until an experiment was completed in order to analyze all the samples in a single run (see SI for details). Moreover, samples can easily be diluted to obtain identical peak areas and hence to maximize the precision and accuracy of the analysis. Carbon isotope ratios were determined using gas chromatography–isotope ratio mass spectrometry (GC-IRMS), chlorine isotope ratios using a GC quadrupole MS method and taking into account four isotopologues (164, 166, 168, 170) as described in detail in the SI. All isotope ratios were reported relative to a standard (VPDB for carbon and SMOC for chlorine isotope) using the delta notation. The combined standard uncertainty was 0.11‰ for carbon and 0.43‰ for chlorine isotopes, and the relative combined standard uncertainty was 9% for concentrations analysis.

Numerical Modeling. The migration of the PCE from the groundwater plume through the capillary fringe and unsaturated zone was simulated using the finite-element code COMSOL Multiphysics. The main goal of the modeling was to gain additional insight into factors that influence the isotope ratios during migration of compounds from the saturated to the unsaturated zone and to extrapolate the results to systems with a different lithology or geometry. Water flow and distribution under variably saturated conditions at steady state were simulated based on Richard's equation. Soil water retention curves were characterized with the Van Genuchten equation.²⁸ The transport of the PCE was assumed to be driven by advection, dispersion, and diffusion in the saturated zone and in the capillary fringe. In the unsaturated zone, only diffusion was assumed to occur. All the parameters except the transverse vertical dispersivity were determined independently. Transverse dispersivity was varied between 0.2 and 5 mm. As no significant variations of isotope ratios were observed in this range of values, a value of 1 mm was chosen for the modeling. A dimensionless Henry coefficient of 0.65 and the isotope fractionation factor air–water partitioning determined in this study were used. The Henry coefficient was determined during air–water partitioning experiments by measuring PCE concentrations in gas and water phase at several equilibration steps (data not shown). The porosity was determined experimentally (see above). The values of Van Genuchten parameters, residual water content and saturated hydraulic conductivity were estimated according to Carsel and Parish²⁹

based on grain size distribution. Diffusion coefficient in the air and water were defined according to Lugg³⁰ and Worch,³¹ respectively. Fractionation between light and heavy isotopologues was quantified using the following equation³² (see SI for more details):

$$\alpha_{\text{Diff}} = \frac{D_h}{D_l} = \sqrt{\frac{(MW_h + MW_m) \cdot MW_l}{(MW_l + MW_m) \cdot MW_h}} \quad (3)$$

where D_h and D_l are the diffusion coefficient for heavy and light isotopologues respectively, MW_l is the molecular weight of the light molecule, MW_h is the molecular weight of the heavy molecule, and MW_m the mass of molecules in the media through which diffusion takes place. Because isotopes and pairs of isotopologues differing in one heavy isotope fractionate the same way, isotope fractionation factors can thus be used to quantify isotopologue fractionation.²⁴ Only the mass 165.83 and 166.83 for carbon isotopes and 165.83 and 167.83 for chlorine isotopes were taken into account for the modeling. Equilibrium was assumed between concentrations in the gas and water phase and only aqueous-phase concentrations are reported. To more easily compare results between the saturated and in the unsaturated zone, experimental results measured in the gas phase were transformed in aqueous values, using Henry's law ($K_{\text{gw}} = 0.65$) and isotope fractionation factors for air–water partitioning determined in this study. More details of the modeling approach and the values of the parameters used for the modeling study (Table S1) can be found in the SI.

RESULTS AND DISCUSSION

Air–Water Partitioning. Significant chlorine and carbon isotope fractionation occurs during air–water partitioning (Figure 1). The isotope evolution during air–water partitioning

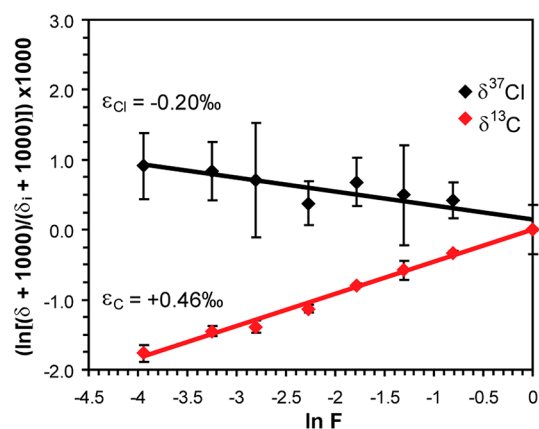


Figure 1. Rayleigh plots for air–water partitioning illustrating concentrations measured in the aqueous phase.

of chlorinated compound follows a Rayleigh trend and isotope enrichment factors are calculated with eqs 1 and 2. As duplicate experiments show similar results, the average values will be discussed here. Chlorine and carbon isotopes show opposite fractionation trends, with a normal isotope effect for chlorine isotopes (enrichment of heavy isotopes in gas phase) and an inverse isotope effect for carbon isotopes (depletion of heavy isotopes in gas phase) (Figure 1). The chlorine isotope enrichment factor for air–water partitioning has a value of $\epsilon_{\text{Cl}} = -0.20 \pm 0.04\text{‰}$, while the enrichment factor for the carbon has a value of $\epsilon_{\text{C}} = +0.46 \pm 0.04\text{‰}$ (Figure 1).

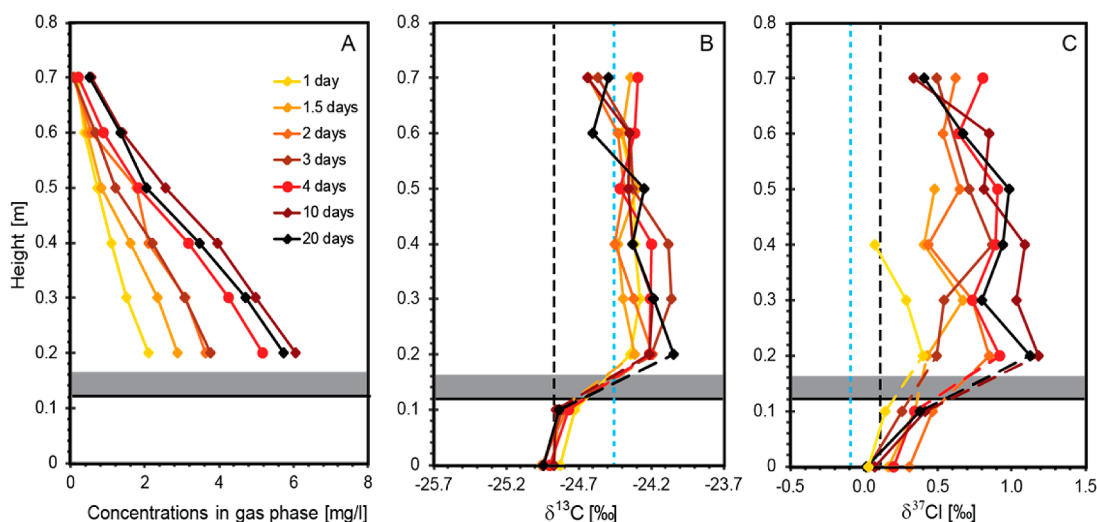


Figure 2. Concentration (A), $\delta^{13}\text{C}$ (B), and $\delta^{37}\text{Cl}$ (C) of PCE in the saturated and unsaturated zone (values for gas phase) of the 2D system (combined standard uncertainty $\pm 0.1\text{‰}$ for C and $\pm 0.43\text{‰}$ for Cl). The horizontal black lines illustrate the location of the water table and the gray lines the extension of the observed capillary fringe. The dashed lines indicate the isotope ratio of dissolved PCE (dashed black) and of gaseous PCE in equilibrium with dissolved PCE (dotted blue).

These results agree with the isotopic fractionation trends observed by Jeannotat and Hunkeler²⁴ for TCE, which showed the same opposite trends for carbon and chlorine isotope fractionation. The enrichment factors are higher for PCE than for TCE ($\epsilon_{\text{Cl}} = -0.20 \pm 0.04\text{‰}$ vs $-0.06 \pm 0.05\text{‰}$ and $\epsilon_{\text{C}} = +0.46 \pm 0.04\text{‰}$ vs $+0.38 \pm 0.04\text{‰}$, respectively). Bacsik et al.³³ and Costa-Gomez and Grolier³⁴ have also measured opposite enrichment factors for carbon and hydrogen isotopes of methane during air–water partitioning, with a normal isotope effect for hydrogen and an inverse isotope effect for carbon isotopes with respect to the gas phase.³³ Jansco and Van Hook^{35,36} have shown that hindered translations and rotations (external mode) will always lead to a normal isotope effect. In contrast, the frequencies of the internal vibrations (internal mode) will in most cases shift toward lower frequencies (red shift) upon dissolution of molecules, leading to an inverse isotope effect. The observed trends for PCE indicate that changes in the internal modes control isotope fractionation for carbon, whereas for chlorine changes in the external modes dominate.

Transport of PCE through the Capillary Fringe and the Unsaturated Zone: Laboratory Experiments and Numerical Modeling. During the first 4 days of the experiment, concentrations in the gas phase steadily increased (Figure 2a). After 4 days, concentrations increased more slowly indicating that a steady state was approached (Figure 2a). The small increase of concentrations from 4 to 20 days observed in Figure 2a is due to a concentration increase in the top of the column, where PCE vapors did not seem to be evacuated efficiently enough to keep concentrations close to 0. The aqueous-phase concentrations at the water table reach 180 mg/L at steady state (data not shown). In the lowest gas-phase sampling point, the gas-phase concentration after 20 days is 20 times smaller with respect to the aqueous-phase concentration at the water table (Figure 2a). This large decrease of concentrations is consistent with similar experiments carried out with TCE by McCarthy and Johnson,¹¹ where very low concentrations were found in the unsaturated zone compared to groundwater. Upward transport across the capillary fringe is restricted compared to transport in the unsaturated zone above,

as diffusion in water is slower than in the gas phase and as the vertical transverse dispersivity in water is small. As a result, at steady state, a steep concentration gradient is established across the capillary fringe compared to the unsaturated zone above to maintain a constant mass flux in vertical direction.

Isotope profiles in the unsaturated zone do not vary with distance from the water table at a given time (Figure 2b and c). However, the chlorine isotopic ratios globally tend to shift to more positive values over time. Carbon and chlorine isotopic ratios thus show only small variations in the unsaturated zone, even at transient state (Figure 2b and c). This contrasts with previous results for diffusion from a NAPL source where a strong depletion of heavy isotopes with distance from a TCE source was observed during the transient expansion of a vapor plume at a similar length scale.²⁴ When substances diffuse out of the water, it takes more time to reach a steady state due to the mass transfer resistance of the capillary fringe which was absent in case of the NAPL source. Hence the isotope profiles have time to constantly readjust, which is not the case during rapid NAPL vaporization. This conclusion is consistent with the shape of the concentration profiles which are nearly linear even at early times suggesting pseudo-steady-state conditions. After 20 days, a difference of about 0.8‰ was observed between aqueous and gaseous values across the capillary fringe for both carbon and chlorine isotopes, which represent a statistically significant variation ($p < 0.05$ according to Student *t* test). Especially for chlorine, this shift is distinctly different from the expected shift if isotope fractionation were due to air–water partitioning only (blue vertical dotted lines in Figure 2b and c). To evaluate the influence of each physical process (air–water partitioning and diffusion) and their combination on the isotope ratios in the capillary fringe, numerical modeling of the 2D system experiment was performed.

The numerical modeling made it possible to evaluate the effect of different physical processes on isotope fractionation during transport of PCE between the saturated and unsaturated zone, as well as to generalize the findings of the laboratory study by considering different scenarios. To simplify the comparison of isotope ratios from the saturated and the unsaturated zone, only aqueous-phase concentrations are

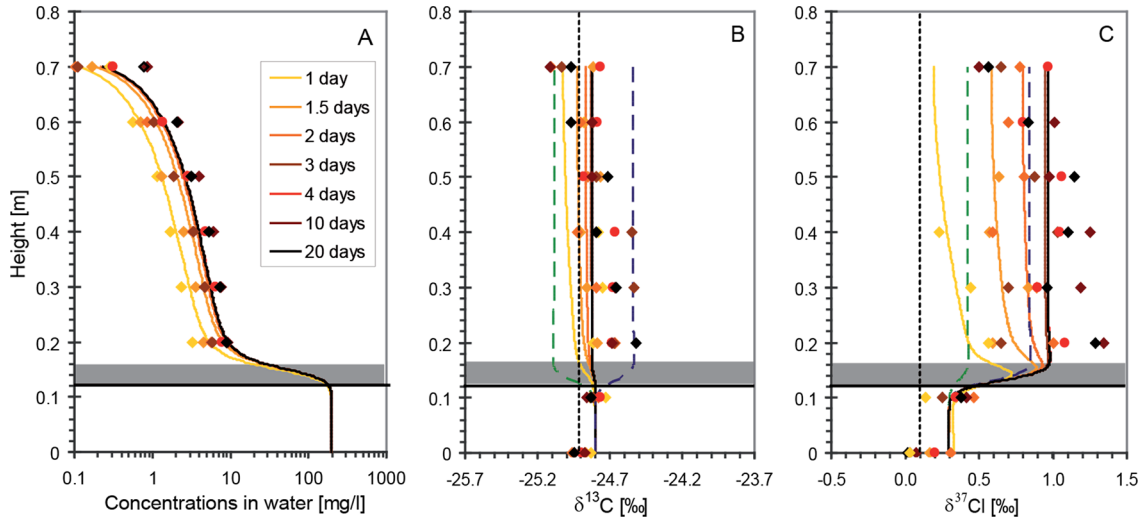


Figure 3. Concentration (A), $\delta^{13}\text{C}$ (B), and $\delta^{37}\text{Cl}$ (C) of measured (points) and modeled (lines) PCE in the middle of the 2D system (combined standard uncertainty $\pm 0.11\text{‰}$ for C and $\pm 0.43\text{‰}$ for Cl). All values correspond to equivalent values in the water phase to obtain continuous curves across the capillary fringe. The lines indicate steady-state isotope ratios with a diffusion isotope effect only (dashed blue), steady state isotope ratios with an air–water partitioning isotope effect only (dashed green), and the isotope ratio of source PCE (dashed black).

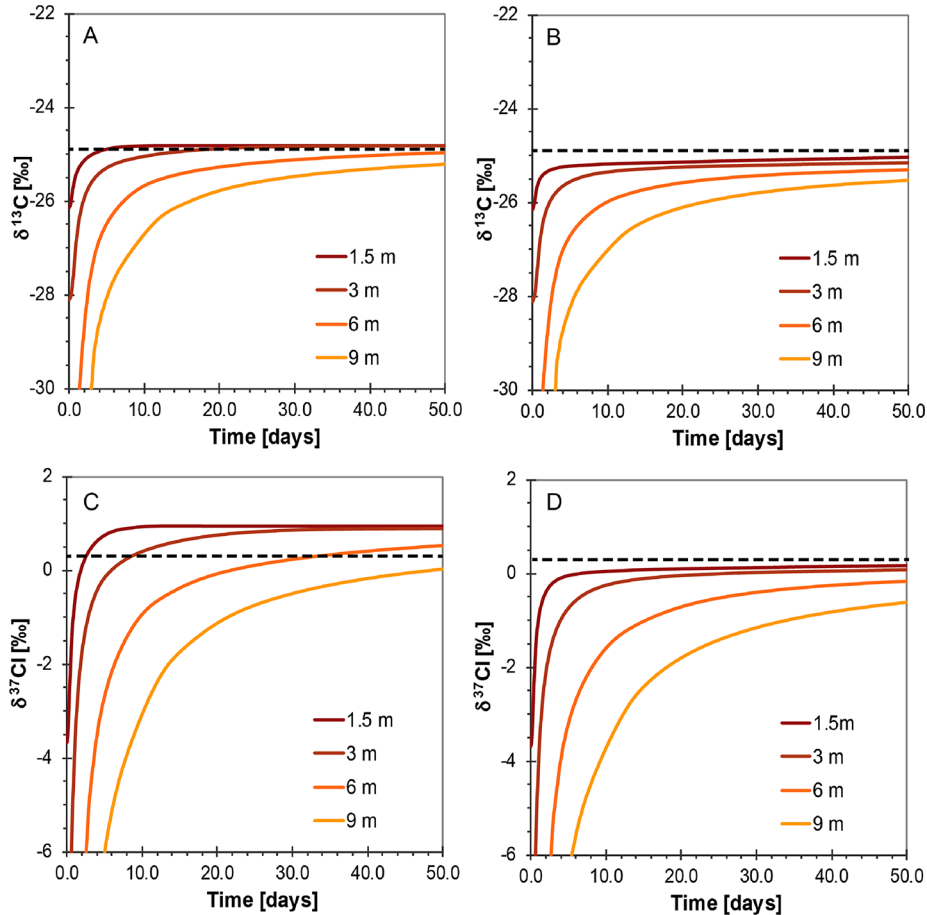


Figure 4. Influence of the thickness of the unsaturated zone and the top boundary conditions (A, C open to atmosphere; B, D closed) on the carbon (A, B) and chlorine (C, D) isotope ratios at 0.5 m below the top of the unsaturated zone. Isotope ratios are expressed as aqueous-phase values.

reported in Figure 3. The same trends are obtained for experimental values and the numerical modeling for both concentrations and isotopic values. Concentration profiles are linear in the unsaturated zone above the capillary fringe and increase over time until a steady state is reached. A strong

concentration gradient is observed in the capillary fringe. The isotope profiles obtained with numerical modeling agree well with experimental results. Only 11% (carbon) or 2% (chlorine) of the measured data deviate by more than 0.5‰ from the modeled data.

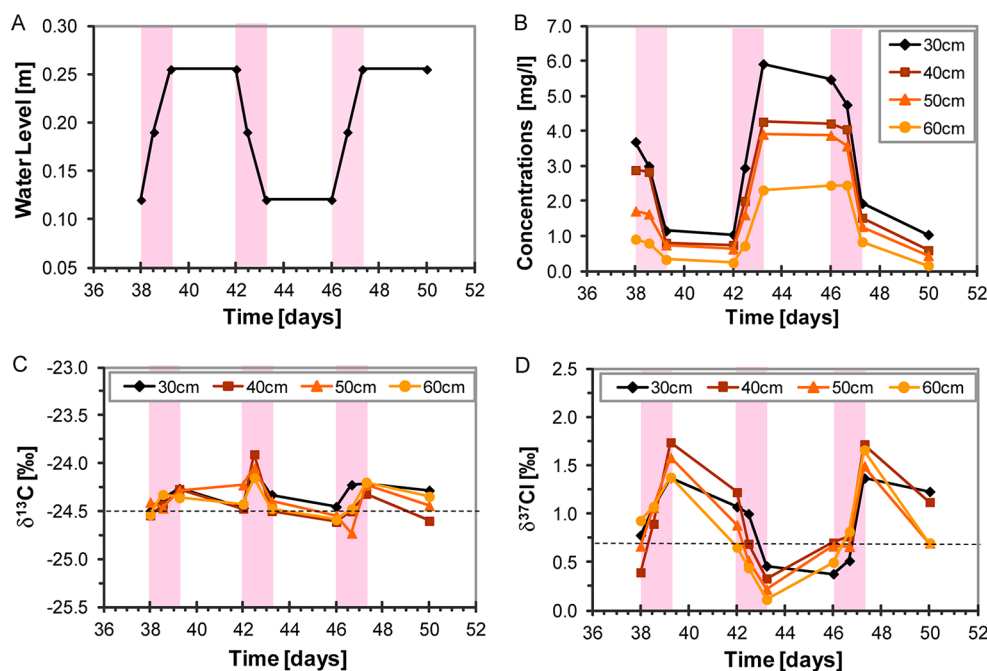


Figure 5. Results of water level fluctuations experiments. Temporal variations of the water level (A), concentrations (B), $\delta^{13}\text{C}$ (C), and $\delta^{37}\text{Cl}$ (D) in the gas phase (combined standard uncertainty $\pm 0.11\text{‰}$ for C and $\pm 0.43\text{‰}$ for Cl). The horizontal lines represent isotopic values at steady state. The red bands correspond to periods when the water table was varied.

In the model, constant isotopic values are obtained at steady state through the unsaturated zone above the capillary fringe. In the case of chlorine isotopes, a small offset of aqueous-phase isotopic values is observed across the capillary fringe (0.7‰) (Figure 3c). In contrast, for carbon the change across the capillary fringe was $<0.1\text{‰}$. The absence of isotope fractionation for carbon in the capillary fringe, but not for chlorine, was explored further using the numerical model. In Figure 3b and c, the dashed blue curves represent the isotopic values at steady state when diffusion only is associated with isotope fractionation (normal isotope effect with $\epsilon = -0.44\text{‰}$ for carbon and $\epsilon = -0.88\text{‰}$ for chlorine, SI eq S8). The dotted green curves represent the isotopic values at steady state with isotope fractionation due to air–water partitioning only (inverse isotope effect with $\epsilon = +0.46\text{‰}$ for carbon and $\epsilon = -0.2\text{‰}$ for chlorine, calculated with eq 3). For carbon isotopes, the normal isotope effect of diffusion is partly canceled by the air–water partitioning isotope effect (black curve of Figure 3b). In contrast, in the case of chlorine isotopes, the normal isotope effect of diffusion and the normal isotope effect for air–water partitioning partly cumulate, leading to a larger enrichment in heavy isotopes in the capillary fringe (black curve of Figure 3c). As the offset observed for chlorine in the aqueous phase of the capillary fringe seems mainly influenced by the fractionation caused by the diffusion (Figure 3c), it is expected to be higher for lighter molecules (diffusion enrichment factor of 1.5‰ for the *cis*-DCE; calculated with eq 3).

Using the numerical model, various scenarios were studied in order to evaluate the effect of the unsaturated zone thickness and the lithology on the isotope evolution. The height of the unsaturated zone was varied between 1.5 and 9 m while maintaining all other factors (Figure 4). For each height two boundary scenarios were simulated, an unsaturated zone open to the atmosphere and an unsaturated zone covered with an impermeable layer (e.g., building or pavement). In Figure 4, the isotope ratios at 0.5 m below the top of the unsaturated zone

are reported mimicking values obtained during shallow soil gas sampling. For all depth and both boundary scenarios, PCE is initially depleted in heavy isotopes and then approaches the isotope signature of the source. The thicker the unsaturated zone is, the larger the initial depletion of heavy isotopes is. After 50 days, isotope ratios deviate less than 1‰ from the source for all scenarios (Figure 4). For open conditions, carbon isotopes converge toward the source value, while chlorine isotopes become enriched in heavy isotopes compared to the source as also observed in the laboratory experiment. PCE with heavy chlorine isotopes is preferentially removed from the unsaturated zone due to the normal isotope effects associated with air–water partitioning and gas-phase diffusion. For carbon, these two effects cancel. For the closed system, both carbon and chlorine isotope ratios approach the source values as no preferential removal of light compounds from the unsaturated zone occurs. The steady state isotope signatures for chlorine are about 0.8‰ apart for open and closed system, while they deviate only by 0.2‰ for carbon.

To explore in more detail the factors that control the isotope patterns, additional simulations were made for the 3 meters scenario (open to atmosphere) with only one process that fractionates isotopes (either gas-phase diffusion or air–water partitioning). These simulations demonstrate that the isotope trends in the unsaturated zone under transient conditions are dominated by isotope fractionation associated with gas-phase diffusion (SI Figure S2).

In addition, the effect of different lithologies (from sand to sandy clay) was explored based on the 0.8 m 2D system. Values of porosity, residual water content, hydraulic conductivity and Van Genuchten parameters (SI Table S2) were chosen according to values given by Carsel and Parrish.²⁹ The finer the grain size is, the higher the initial depletion of heavy isotopes is (SI Figure S3). However, after 50 days, the isotope ratios deviate less than 1‰ from the source value.

Whereas constant isotopic profiles are reached at steady state throughout the unsaturated zone above the capillary fringe, how will isotopic ratios evolve for more dynamic environmental conditions? To address this question the water table was changed several times in a period of 15 days. The water level was increased from 0.12 to 0.25 m at 9 cm/day, stabilized during 3 days, lowered at the same rate and to the initial water table, stabilized during 3 days, and finally increased back to a level of 0.25 m (Figure 5a). When the water level increases, the concentrations in the unsaturated zone decrease (Figure 5b). Conversely, during water table drop, concentrations increase considerably in the unsaturated zone. The concentrations decrease again when the water table is raised for the second time. All the variations of concentrations fit quite well with previous experiments by McCarthy and Johnson¹¹ that investigated effects of water table changes and the same trends are observed.

During water table fluctuations, carbon isotope ratios vary less (amplitude of 0.65‰ for a given sampling point) than chlorine isotopes (amplitude of 1.5‰ for a given sampling point). When the water level increases, PCE becomes more enriched in ³⁷Cl, and when water level drops, it becomes more depleted. The isotope ratio of PCE in the unsaturated zone depends on the rate of loss of molecules via diffusion through the unsaturated zone, which preferentially removes light molecules. In addition, it is influenced by the rate of transfer of molecules from the aqueous to the gaseous phase which is less isotope sensitive (as air–water partitioning is small and the aqueous phase is continuously replenished by the flow) or which might deliver preferentially light isotopes due to isotope fractionation associated with aqueous-phase diffusion. During the water table fluctuation, the balance between the two factors is disturbed. When the water level rises, fewer molecules are transferred from the water to the gas phase as indicated by the lower concentrations. As light isotopes diffuse out of the system faster, a depletion of light isotopes occurs in the capillary fringe. Chlorine isotopes thus show variations of 1.5‰ during the 13 cm water table fluctuations. However, because transport in the gas phase is rapid, the $\delta^{37}\text{Cl}$ values tend to reverse to the steady state values after 3 days if the water level is stabilized. When the water level drops, the gas phase close to the water table comes in contact with water containing a high amount of PCE, leading to a temporary increase of concentrations in the gas phase. As the delivery of lighter molecules thus increases, at least temporarily, isotope fractionation drops and $\delta^{37}\text{Cl}$ values become closer to source values. Conversely, carbon isotopes do not show significant variations during water table fluctuations since isotopic fractionation associated with gas-phase diffusion is smaller than for chlorine and is counteracted by inverse isotope fractionation associated with air–water partitioning.

■ IMPLICATIONS FOR FORENSICS STUDIES

A strong deviation of the unsaturated zone VOC isotope ratios from groundwater ratios mainly occurs during the transient migration of VOCs across the unsaturated zone. As a steady state is approached, the isotope ratios converge toward the isotope ratio of dissolved compounds in the saturated zone. For thicker unsaturated zones and less permeable sediments, the depletion in heavy isotopes persists longer. For the scenarios considered in this study (unsaturated zone thickness of up to 9 m), a period of 50 days was sufficient to reach isotope values that deviate less than 1‰ from the groundwater values. Even at

steady state, a small offset between unsaturated zone and groundwater isotope ratios can persist that however remains below 1‰ for the scenarios considered in this study. The offset is due to the isotope effect associated with air–water partitioning and diffusion. The offset is larger for conditions open to the atmosphere, leading to preferential loss of light isotopologues than for a closed boundary (e.g., pavement). Moreover, chlorine isotope variations occur in the unsaturated zone during water table fluctuations. Hence, potential isotope variations due to nonsteady state conditions should be considered when applying CSIA methods at field sites, especially if the unsaturated zone is thick, if layers of fine sediments are present at the site, or if large and rapid water table variations occur. However, at steady state, stable isotope analysis can be used to link a soil gas contamination of chlorinated solvents to a plume located in groundwater as offsets are expected to be small as long as no biodegradation occurs. In fact, similarly as in the saturated zone, biodegradation can lead to an enrichment of heavy isotopes in the unsaturated zone.

■ ASSOCIATED CONTENT

📄 Supporting Information

Additional information about modeling approach. Parameters used during the numerical modeling study. Setup used for the aquifer model experiments. Influence of isotope effect associated with different processes on isotope trends. Effect of lithology on isotope trends. This material is available free of charge via the Internet at <http://pubs.acs.org>.

■ AUTHOR INFORMATION

Corresponding Author

*Phone: ++41 32 718 25 60; fax: ++41 32 718 26 03; e-mail: Daniel.Hunkeler@unine.ch.

Notes

The authors declare no competing financial interest.

■ ACKNOWLEDGMENTS

The authors acknowledge the Swiss National Science Foundation (SNSF) for their financial support.

■ REFERENCES

- (1) Cotel, S.; Schafer, G.; Barthes, V.; Bausand, P. Effect of density-driven advection on trichloroethylene vapor diffusion in a porous medium. *Vadose Zone J.* **2011**, *10* (2), 565–581.
- (2) Johnson, R. L.; Pankow, J. F. Dissolution of dense chlorinated solvents into groundwater. 2. Source functions for pools of solvents. *Environ. Sci. Technol.* **1992**, *26* (5), 896–901.
- (3) Christophersen, M.; Broholm, M. M.; Mosbaek, H.; Karapanagioti, H. K.; Burganos, V. N.; Kjeldsen, P. Transport of hydrocarbons from an emplaced fuel source experiment in the vadose zone at airbase Vaerlose, Denmark. *J. Contam. Hydrol.* **2005**, *81* (1–4), 1–33.
- (4) Jury, W. A.; Spencer, W. F.; Farmer, W. J. Behavior assessment model for trace organics in soil. 0.1. Model description. *J. Environ. Qual.* **1983**, *12* (4), 558–564.
- (5) Mercer, J. W.; Cohen, R. M. A review of immiscible fluids in the subsurface: Properties, models, characterization and remediation. *J. Contam. Hydrol.* **1990**, *6* (2), 107–163.
- (6) Werner, D.; Hohener, P. Diffusive partitioning tracer test for nonaqueous phase liquid (NAPL) detection in the vadose zone. *Environ. Sci. Technol.* **2002**, *36* (7), 1592–1599.
- (7) Bouchard, D.; Hunkeler, D.; Gaganis, P.; Aravena, R.; Hohener, P.; Broholm, M. M.; Kjeldsen, P. Carbon isotope fractionation during

diffusion and biodegradation of petroleum hydrocarbons in the unsaturated zone: Field experiment at Vaerlose Airbase, Denmark, and modeling. *Environ. Sci. Technol.* **2008**, *42* (2), 596–601.

(8) Conant, B. H.; Gillham, R. W.; Mendoza, C. A. Vapor transport of trichloroethylene in the unsaturated zone: Field and numerical modeling investigations. *Water Resour. Res.* **1996**, *32* (1), 9–22.

(9) Bohy, M.; Dridi, L.; Schafer, G.; Razakarisoa, O. Transport of a mixture of chlorinated solvent vapors in the vadose zone of a sandy aquifer: Experimental study and numerical modeling. *Vadose Zone J.* **2006**, *5* (2), 539–553.

(10) Falta, R. W.; Javandel, I.; Pruess, K.; Witherspoon, P. A. Density-driven flow of gas in the unsaturated zone due to the evaporation of volatile organic-compounds. *Water Resour. Res.* **1989**, *25* (10), 2159–2169.

(11) McCarthy, K. A.; Johnson, R. L. Transport of volatile organic-compounds across the capillary-fringe. *Water Resour. Res.* **1993**, *29* (6), 1675–1683.

(12) Hunkeler, D.; Chollet, N.; Pittet, X.; Aravena, R.; Cherry, J. A.; Parker, B. L. Effect of source variability and transport processes on carbon isotope ratios of tce and pce in two sandy aquifers. *J. Contam. Hydrol.* **2004**, *74* (1–4), 265–282.

(13) Blessing, M.; Schmidt, T. C.; Dinkel, R.; Haderlein, S. B. Delineation of multiple chlorinated ethene sources in an industrialized area—A forensic field study using compound-specific isotope analysis. *Environ. Sci. Technol.* **2009**, *43* (8), 2701–2707.

(14) Jendrzewski, N.; Eggenkamp, H. G. M.; Coleman, M. L. Characterisation of chlorinated hydrocarbons from chlorine and carbon isotopic compositions: Scope of application to environmental problems. *Appl. Geochem.* **2001**, *16* (9–10), 1021–1031.

(15) Shouakar-Stash, O.; Frape, S. K.; Drimmie, R. J. Stable hydrogen, carbon and chlorine isotope measurements of selected chlorinated organic solvents. *J. Contam. Hydrol.* **2003**, *60* (3–4), 211–228.

(16) Hunkeler, D.; Aravena, R.; Butler, B. J. Monitoring microbial dechlorination of tetrachloroethene (PCE) in groundwater using compound-specific stable carbon isotope ratios: Microcosm and field studies. *Environ. Sci. Technol.* **1999**, *33* (16), 2733–2738.

(17) Lollar, B. S.; Slater, G. F.; Sleep, B.; Witt, M.; Klecka, G. M.; Harkness, M.; Spivack, J. Stable carbon isotope evidence for intrinsic bioremediation of tetrachloroethene and trichloroethene at Area 6, Dover Air Force Base. *Environ. Sci. Technol.* **2001**, *35* (2), 261–269.

(18) Meckenstock, R. U.; Morasch, B.; Griebler, C.; Richnow, H. H. Stable isotope fractionation analysis as a tool to monitor biodegradation in contaminated aquifers. *J. Contam. Hydrol.* **2004**, *75* (3–4), 215–255.

(19) Hunkeler, D.; Abe, Y.; Broholm, M. M.; Jeannotat, S.; Westergaard, C.; Jacobsen, C. S.; Aravena, R.; Bjerg, P. L. Assessing chlorinated ethene degradation in a large scale contaminant plume by dual carbon-chlorine isotope analysis and quantitative PCR. *J. Contam. Hydrol.* **2010**, *119* (1–4), 69–79.

(20) Poulson, S. R.; Drever, J. I. Stable isotope (C, Cl, and H) fractionation during vaporization of trichloroethylene. *Environ. Sci. Technol.* **1999**, *33* (20), 3689–3694.

(21) Wang, Y.; Huang, Y. S. Hydrogen isotopic fractionation of petroleum hydrocarbons during vaporization: Implications for assessing artificial and natural remediation of petroleum contamination. *Appl. Geochem.* **2003**, *18* (10), 1641–1651.

(22) Bouchard, D.; Hohener, P.; Hunkeler, D. Carbon isotope fractionation during volatilization of petroleum hydrocarbons and diffusion across a porous medium: A column experiment. *Environ. Sci. Technol.* **2008**, *42* (21), 7801–7806.

(23) Kuder, T.; Philp, P.; Allen, J. Effects of volatilization on carbon and hydrogen isotope ratios of MTBE. *Environ. Sci. Technol.* **2009**, *43* (6), 1763–1768.

(24) Jeannotat, S.; Hunkeler, D. Chlorine and carbon isotopes fractionation during volatilization and diffusive transport of trichloroethene in the unsaturated zone. *Environ. Sci. Technol.* **2012**, *46* (6), 3169–3176.

(25) Hunkeler, D.; Aravena, R.; Shouakar-Stash, O.; Weisbrod, N.; Nasser, A.; Netzer, L.; Ronen, D. Carbon and chlorine isotope ratios of chlorinated ethenes migrating through a thick unsaturated zone of a sandy aquifer. *Environ. Sci. Technol.* **2011**, *45* (19), 8247–8253.

(26) Bradley, P. M. Microbial degradation of chloroethenes in groundwater systems. *Hydrogeol. J.* **2000**, *8* (1), 104–111.

(27) Haberer, C.; Rolle, M.; Liu, S.; Cirpka, O. A.; Grathwohl, P. A high-resolution non-invasive approach to quantify oxygen transport across the capillary fringe and within the underlying groundwater. *J. Contam. Hydrol.* **2011**, *122*, 26–30.

(28) van Genuchten, M. T. A closed-form equation for predicting the hydraulic conductivity of unsaturated soils. *Soil Sci. Soc. Am. J.* **1980**, *44* (5), 892–898.

(29) Carsel, R. F.; Parrish, R. S. Developing joint probability-distributions of soil-water retention characteristics. *Water Resour. Res.* **1988**, *24* (5), 755–769.

(30) Lugg, G. A. Diffusion coefficients of some organic and other vapors in air. *Anal. Chem.* **1968**, *40* (7), 1072–1077.

(31) Worch, E. Eine neue Gleichung zur Berechnung von Diffusionskoeffizienten gelöster Stoffe. *Vom Wasser* **1993**, *81*, 289–297.

(32) Craig, H. The geochemistry of the stable carbon isotopes. *Geochim. Cosmochim. Acta* **1953**, *3* (2–3), 53–92.

(33) Bacsik, Z.; Lopes, J. N. C.; Gomes, M. F. C.; Jancso, G.; Mink, J.; Padua, A. A. H. Solubility isotope effects in aqueous solutions of methane. *J. Chem. Phys.* **2002**, *116* (24), 10816–10824.

(34) Gomes, M. F. C.; Grolier, J. P. Determination of Henry's law constants for aqueous solutions of tetradeuteriomethane between 285 and 325 K and calculation of the H/D isotope effect. *Phys. Chem. Chem. Phys.* **2001**, *3* (6), 1047–1052.

(35) Jancso, G.; Vanhook, W. A. Condensed phase isotope-effects (especially vapor-pressure isotope-effects). *Chem. Rev.* **1974**, *74* (6), 689–750.

(36) Jancso, G. Interpretation of isotope effects on the solubility of gases. *Nukleonika* **2002**, *47*, S53–S57.